CHARACTERIZATION OF MECHANICAL AND IN-SITU FRACTURE BEHAVIORS OF REACTION SQUEEZE CAST HYBRID AL MATRIX COMPOSITES

Changook Son[1], Ikmin Park[1], Kyungmox Cho[1], and Ildong Choi[2]

[1]Dept. of Metallurgical Engineering, Pusan National University, Pusan 609-735, Korea
[2]Dept. of Materials Engineering, Korea Maritime University, Pusan 606-791, Korea

SUMMARY: Mechanical properties of ($10\%Al_2O_3$• SiO_2+5%Ni)/Al and ($10\%Al_2O_3$• SiO_2+5%TiO_2)/Al hybrid composites fabricated by the reaction squeeze casting were compared with those of ($15\%Al_2O_3$• SiO_2)/Al composites. Al-Ni and Al-Ti intermetallic compound formed by the reaction between molten aluminum and reinforcing powder were uniformly distributed in the Al matrix. These intermetallic compounds were identified as Al_3Ni and Al_3Ti using EDS and X-ray diffraction analysis and they enhanced room and high temperature strength. While tensile and yield strength of hybrid composites were greater at room temperature and 300°C than those of ($15\%Al_2O_3$• SiO_2)/Al composites, strength drop at high temperature was much smaller in hybrid composites. It was identified from the in-situ fracture test of ($15\%Al_2O_3$• SiO_2)/Al composites, microcracks were initiated mainly at the short fiber / matrix interfaces. As the loading was continued, the crack propagated mainly along the separated interfacial regions and the well developed shear bands. It was identified from the in-situ fracture test of ($10\%Al_2O_3$• SiO_2+5%Ni)/Al hybrid composites, microcracks were initiated mainly by the short fiber / matrix interfacial debonding. As the loading was continued, the crack proceeded mainly through the intermetallic compound clusters.

KEY WORDS: hybrid MMC, reaction squeeze casting, intermetallic compound, mechanical properties, in-situ fracture test.

INTRODUCTION

Al matrix composites have appeared as the key structural materials not only in the fields of aeronautic and aerospace industries but also in the general industrial field. The automobile industry will be one of the great targets for the composites, which have excellent mechanical properties upto elevated temperature in addition to light weight. However, the application of Al alloy metal matrix composites for automotive parts has been limited due to the softening of Al matrix and interfacial reaction between matrix and reinforcement at the high temperature (more than 300 °C)[1-4]. Recently the new reaction squeeze casting techniques have been proposed to overcome the deterioration of Al matrix at high temperatures. Intermetallic compounds formed by the reaction between aluminum melt and the metal powder(Fe,Cu,Ni) or the metal oxide powder(TiO_2, NiO) during the squeeze casting are very effective for improving the mechanical properties such as hardness, wear resistance, and high temperature strength[5-6]. Reaction squeeze casting which is newly applied to form intermetallic compounds has advantages of low cost, simple process, low product defects, mass productivity of near-net-shape parts, and save energy(form easily intermetallic compounds near the melting point of low melting metal).

In the present study, (10%Al_2O_3• SiO_2+5%Ni)/Al and (10%Al_2O_3• SiO_2+5%TiO_2)/Al hybrid composites were fabricated by the reaction squeeze casting. Microstructure has been analyzed and mechanical properties have been characterized for hybrid composites. Microstructure and mechanical properties of (15%Al_2O_3• SiO_2)/Al composites and pure Al have been also analyzed for comparison. In- situ fracture tests were conducted on (15%Al_2O_3• SiO_2)/Al composites and (10%Al_2O_3• SiO_2+5%Ni)/Al hybrid composites to identify the microfracture process.

EXPERIMENTAL

Pure aluminum (purity 99.9%) was chosen for matrix. Kaowool short fiber(amorphous structure with average dimensions of 2.8μ in diameter and 20~300μ in length, 47%Al_2O_3-53%SiO_2 : Isolite Co.), Ni powder(purity 99.9%, 2-3μ in diameter) and TiO_2 powder(purity 99.9%, <1μ in diameter, anatase type) were used as reinforcements for the fabrication of reaction squeeze cast (10%Al_2O_3• SiO_2+5%Ni)/Al and (10%Al_2O_3• SiO_2+5%TiO_2)/Al hybrid composites. The hybrid preform was prepared by employing the vacuum suction method. The mixture of reinforcements, silica colloidal inorganic binder, starch organic binder and polyacrylamide was dispersed in distilled water and consolidated with vacuum suction method[7-8].

The aiming volume fraction of reinforcements in the preform(20·32·84mm) was about 15% and roughly controlled with vacuum suction pressure. Preforms were dried at room temperature for 3 days and at 110 ^oC for 7 days in an oven. (10%Al_2O_3• SiO_2+5%Ni)/Al hybrid composites were fabricated by infiltrating the molten aluminum of 750 ^oC, 800 ^oC, 850 ^oC and 900 ^oC into the hybrid preform placed in the high speed steel mold preheated to 400 ^oC and (10%Al_2O_3• SiO_2+5%TiO_2)/Al hybrid composite was fabricated by infiltrating the molten aluminum of 800 ^oC into the hybrid preform placed in the mold preheated to 400 ^oC. The temperature of the molten aluminum in (10%Al_2O_3• SiO_2+5%Ni)/Al hybrid composites was varied to see the effect of temperature on the formation of intermetallic compounds. Preforms were also heated to 400^oC to improve the wettability between matrix and reinforcements. During infiltrating molten aluminum into the hybrid preform, 35MPa was applied within 7 seconds, and was held for 60 seconds[9-11].

SEM-EDS and XRD analyses were carried out to investigate the microstructure of the composites. Microhardness test, three-point bending test and tensile test of the composites fabricated by infiltrating the molten aluminum of 800 ^oC were performed to characterize the mechanical properties. Tensile test was carried out at 25øC and 300øC to evaluate high temperature properties of composites.

In-situ SEM fracture test for direct observation of the fracture process was conducted using a compact tension (CT) type loading stage. Dimension of CT type specimen was 10·9.6mm with a thickness of 0.5mm in the grooved section and sharp notch (about 75μ radius) was introduced by electro-discharge machine. At each loading step, the stress intensity factor was measured with the monitored load cell (the maximum load: 20kgf) which was connected to the X-Y recorder. Apparent fracture toughness (K_A) test and data interpretation procedures followed ASTM E399 specification[12-15].

RESULTS AND DISCUSSION

Microstructure

Fig. 1 shows SEM microstructures of (15%Al_2O_3• SiO_2)/Al composite, (10%Al_2O_3• SiO_2+5%Ni)/Al and (10%Al_2O_3• SiO_2+5%TiO_2)/Al hybrid composites fabricated by the infiltration of molten aluminum of 800øC to the preforms. Composites reveal uniform

distribution of reinforcements and no visible casting defects. In hybrid composites, Al-Ni and Al-Ti intermetallic compounds are formed through the reaction between reinforcements molten aluminum. Microstructural investigation shows that (10%Al_2O_3• SiO_2+5%Ni)/Al hybrid composite has relatively more intermetallic compounds than (10%Al_2O_3• SiO_2+5%TiO_2)/Al hybrid composite. It is considered that the difference in the quantity of reaction products is caused by the reactivity between Al matrix and reinforcement powder. That is, Ni powder is more reactive with molten aluminum than TiO_2 powder. Al_3Ni, Al_3Ni_2 or AlNi intermetallic compounds can be formed by the reaction with molten aluminum of 750øC-900øC according to the Al-Ni phase diagram[16]. The SEM-EDS analysis of (10%Al_2O_3• SiO_2+5%Ni)/Al hybrid composite in Figure 2 shows that the amount of Ni is increased from 4.0at% at Al matrix(point A) up to 23.3at% at the center of intermetallic compound(point C). Therefore, it could be concluded that main reaction product is Al_3Ni intermetallic compound.

The X-ray diffraction patterns of (10%Al_2O_3• SiO_2+5%Ni)/Al hybrid composite in Fig. 3 show peaks of the Al_3Ni without any peak of other compounds regardless of the pouring temperatures of the molten aluminum. It can be seen from Al-Ni binary phase diagram[16] that Al_3Ni might be easily formed comparing to the other Al-Ni intermetallic compounds due to its lower formation temperature.

The SEM-EDS analysis of (10%Al_2O_3• SiO_2+5%TiO_2)/Al hybrid composite in Figure 4 shows that the amount of Ti is increased from 7.0at% at Al matrix(point A) up to 31.0at% at the center of intermetallic compound(point C). The fraction of Ti in the Al-Ti compound is measured about 31%, and thus the reaction product is found as Al_3Ti. The X-ray diffraction patterns of (10%Al_2O_3• SiO_2+5%TiO_2)/Al hybrid composites in Fig. 5 reveal peaks of Al_2O_3 as well as Al_3Ti. It can be seen from Al-Ti binary phase diagram[17] that Al_3Ti might be easily formed comparing to the other Al-Ti intermetallic compound due to its lower formation temperature.

Mechanical Properties

The results of the microhardness test and three-point bending test are summarized in Fig. 6 for squeeze cast Al, (15%Al_2O_3• SiO_2)/Al composite, (10%Al_2O_3• SiO_2+5%Ni)/Al and (10%Al_2O_3• SiO_2+5%TiO_2)/Al hybrid composites with pouring temperature of molten aluminum of 800^{o}C. Microhardness and flexural strength of hybrid composites is higher than that of (15%Al_2O_3• SiO_2)/Al composite. These enhancements of mechanical properties, such as microhardness and flexural strength are likely to be increased due to the hard intermetallic compound particles.

Tensile tests were performed to evaluate the composite strength at room and elevated temperature. All tensile-test data are summarized in Table 1. It shows that tensile and yield strength of hybrid composites are greater than (15%Al_2O_3• SiO_2)/Al composite at both temperatures(25 ^{o}C, 300 ^{o}C). Strength drop at 300 ^{o}C is much smaller in hybrid composites. The relatively less drop of the strength at elevated temperature in hybrid composites could be caused by the stability of the intermetallic compounds.

Tensile properties of (10%Al_2O_3• SiO_2+5%Ni)/Al hybrid composite are superior to that of (10%Al_2O_3• SiO_2+5%TiO_2)/Al hybrid composite at room temperature and 300 ^{o}C. The difference of mechanical properties is due to the amount of reaction product. Microstructural investigation in Fig. 1 showed that (10%Al_2O_3• SiO_2+5%Ni)/Al hybrid composite had more intermetallic compounds than (10%Al_2O_3• SiO_2+5%TiO_2)/Al hybrid composite.

Fig. 1: SEM microstructure of squeeze cast Al matrix composites with pouring molten

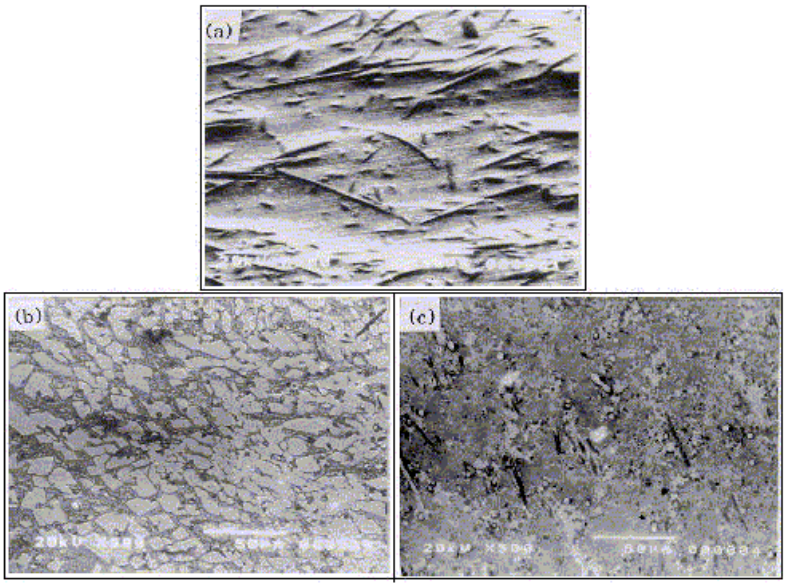

aluminum of 800 ∅ C : (a) (15%Al_2O_3· SiO_2)/Al, (b) (10%Al_2O_3· SiO_2+5%Ni)/Al , (c) (10%Al_2O_3· SiO_2+5%TiO_2)/Al.

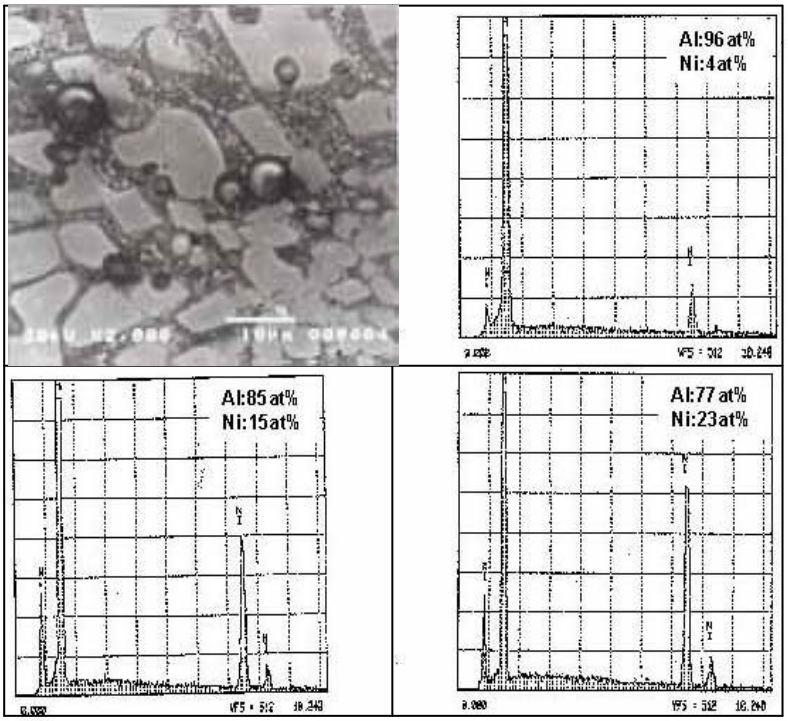

`

Fig. 2: SEM-EDS analysis of (10%Al_2O_3· SiO_2 + 5%Ni)/Al composite : (a) SEM micrograph (´ 2000), (b) EDS scan of A, (c) EDS scan of B, (d) EDS scan of C.

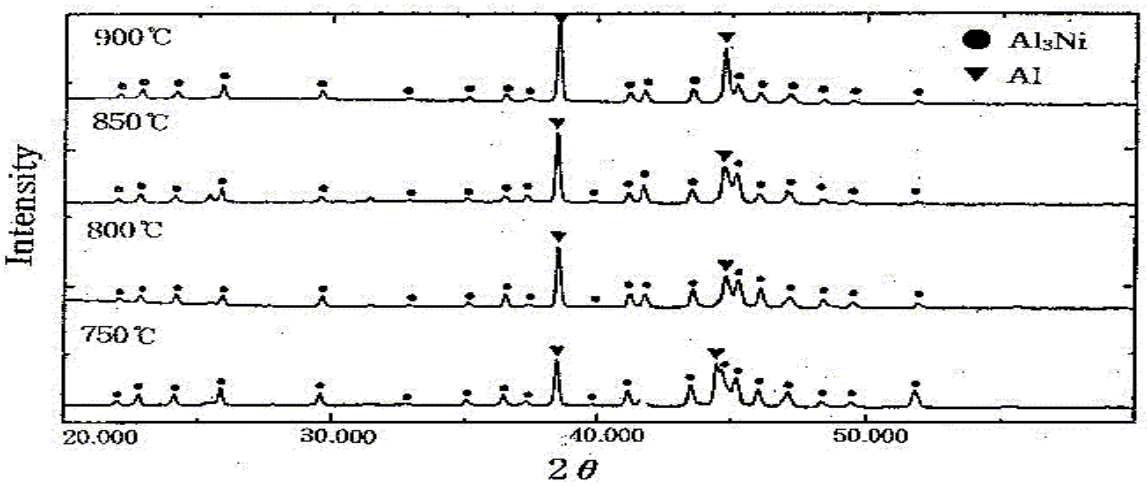

Fig. 3: X-ray diffraction patterns of (10%Al_2O_3· SiO_2 + 5%Ni) / Al hybrid composite according to pouring temperature of molten aluminum.

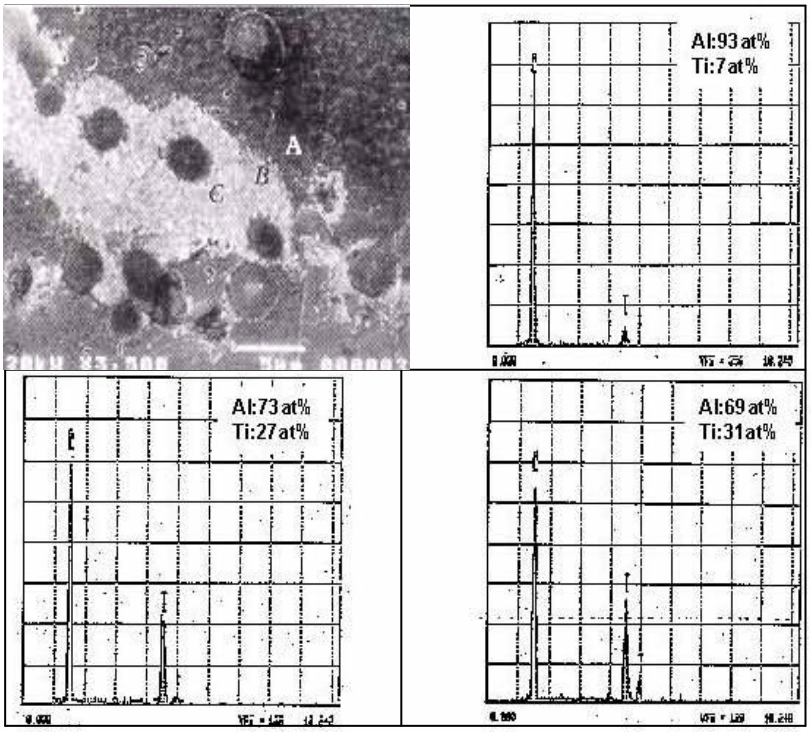

Fig. 4: SEM-EDS analysis of (10%Al_2O_3· SiO_2 + 5%TiO_2) / Al composites
(a) SEM micrograph(´3500), (b) EDS scan of A, (c) EDS scan of B, (d) EDS scan of C.

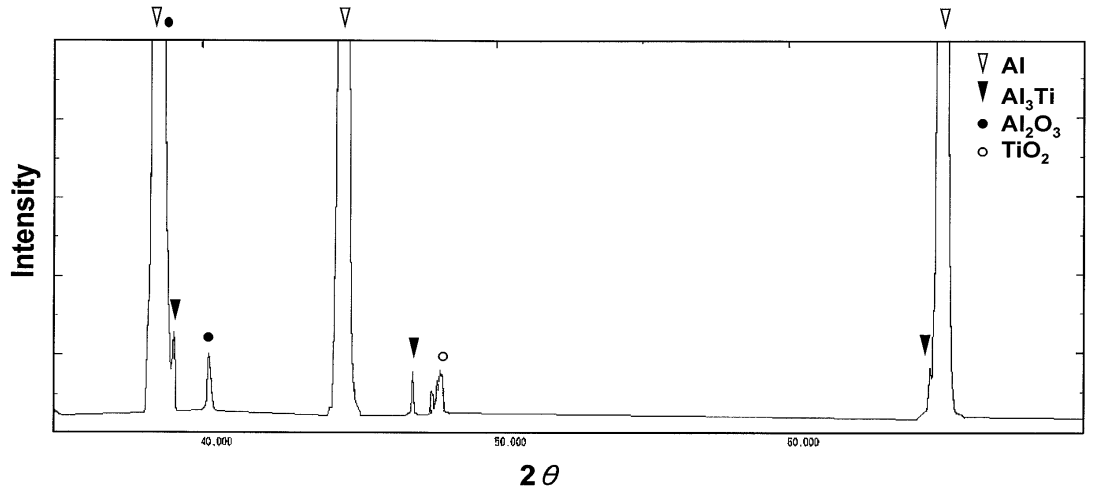

Fig. 5: X-ray diffraction patterns of (10%Al_2O_3· SiO_2 + 5%TiO_2) / Al hybrid composite with pouring temperature of molten aluminum of 800°C.

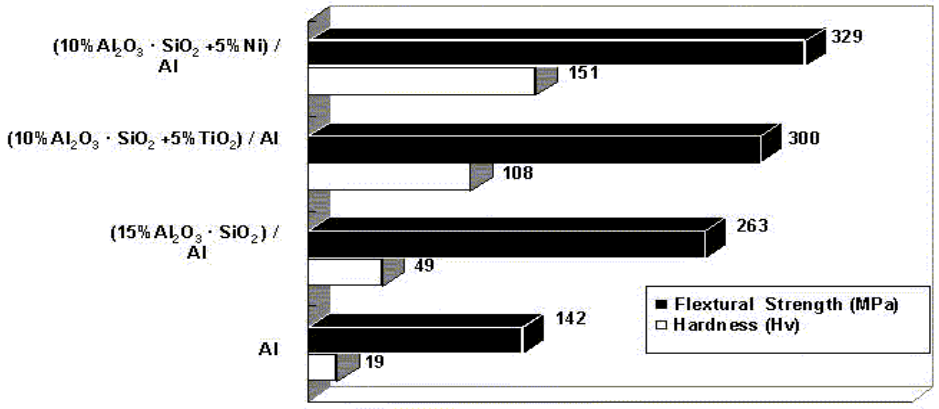

Fig. 6: Hardness(Hv) and flexural strength(MPa) of squeeze cast Al and Al matrix composites.

Table 1: The results of tensile test of the Al matrix composites at the 25°C and 300°C.

Composites	0.2% Y.S.(MPa)		U.T.S.(MPa)		Elongation (%)	
	25 °C	300 °C	25 °C	300 °C	25 °C	300 °C
(15%Al_2O_3• SiO_2)/Al	83	52	118	89	5	9
(10%Al_2O_3•SiO_2+5%TiO_2)/Al	121	112	129	118	2.2	4.4
(10%Al_2O_3• SiO_2+5%Ni)/Al	130	123	135	130	1.2	2.3

In-Situ Observation of Fracture Process

The in-situ observations of fracture behavior for (15%Al_2O_3• SiO_2)/Al composite and (10%Al_2O_3• SiO_2+5%Ni)/Al hybrid composite are made with reference to a series of SEM micrographs in Fig. 7 and Fig. 8, respectively. Fig. 7(a) shows the feature near the notch tip of CT specimen at the initial stage of loading (stress intensity factor (K_Q) = 8.5MPa$\sqrt{m}$). The separation of fiber/matrix interface occurs at several places. As the loading reaches to K_Q=10.9MPa$\sqrt{m}$, Fig. 7(b) reveals the local plastic deformation (shear band) in Al matrix and voids formed at the tips of fibers. Some evidence of the connection of microcracks especially near the notch tip can be observed. Crack propagation with continued loading shown in Fig. 7(c) proceeds along microcracks formed at fiber/matrix interfaces and shear bands formed at ligament region of Al matrix between fibers. Voids at fiber tips and broken sites of fibers also involve the propagation of crack. For the case of (10%Al_2O_3• SiO_2+5%Ni)/Al hybrid composite as shown in Fig. 8(a), defect initiation sites are fiber/matrix and intermetallic/matrix interfaces and fiber tips at early stage of loading (K_Q = 10.76MPa$\sqrt{m}$). Microstructure of the hybrid composite reveals high volume fraction of intermetallic composite particle clusters. Fig. 8(b) shows the well developed cracks in the clusters resulting from the connection of debonded intermetallic/matrix interfaces with loading of K_Q=11.16MPa$\sqrt{m}$. Shear band formation in (10%Al_2O_3• SiO_2+5%Ni)/Al hybrid composite is not so pronounced as in (15%Al_2O_3• SiO_2)/Al composite. Fig. 8(c) shows a long crack developed with continued loading in front of the sharp notch tip of CT specimen, the crack mainly propagates along the intermetallic clusters and fiber/matrix interfaces.

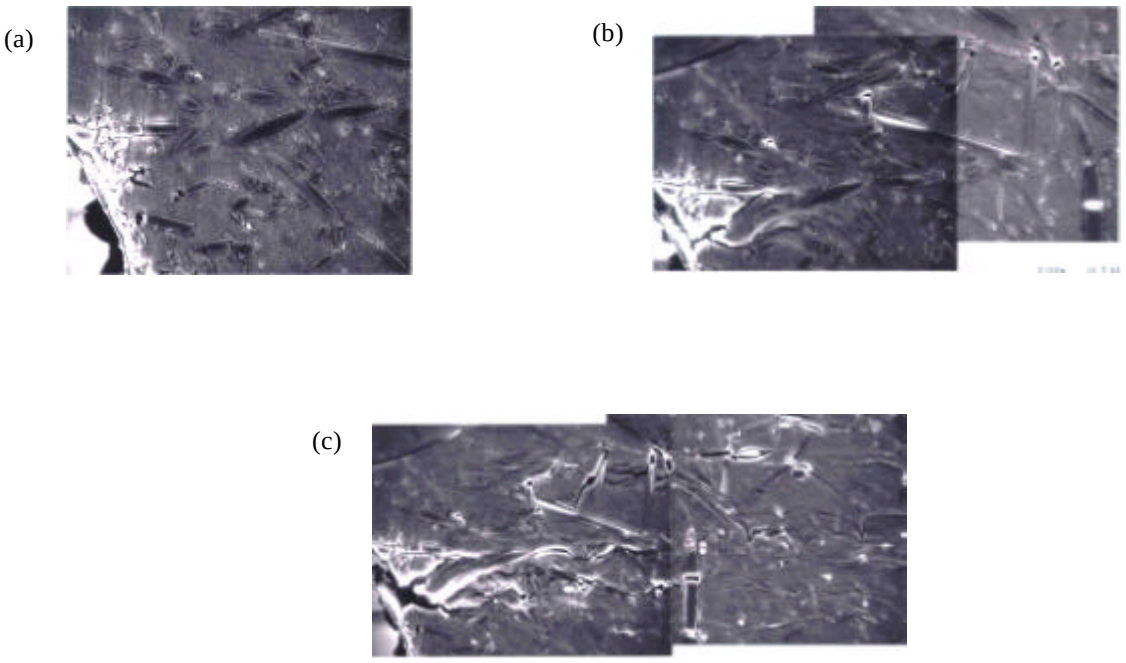

Fig. 7: A series of SEM micrographs near a notch tip of (15%Al_2O_3·SiO_2) / Al composite, showing : (a) microcrack formation by the separation of short fiber / matrix interface(K_Q=8.5 MPa$\sqrt{m}$), (b) (K_Q=10.9 MPa$\sqrt{m}$) and (c) the cracks proceed mainly along the separated interfacial regions.

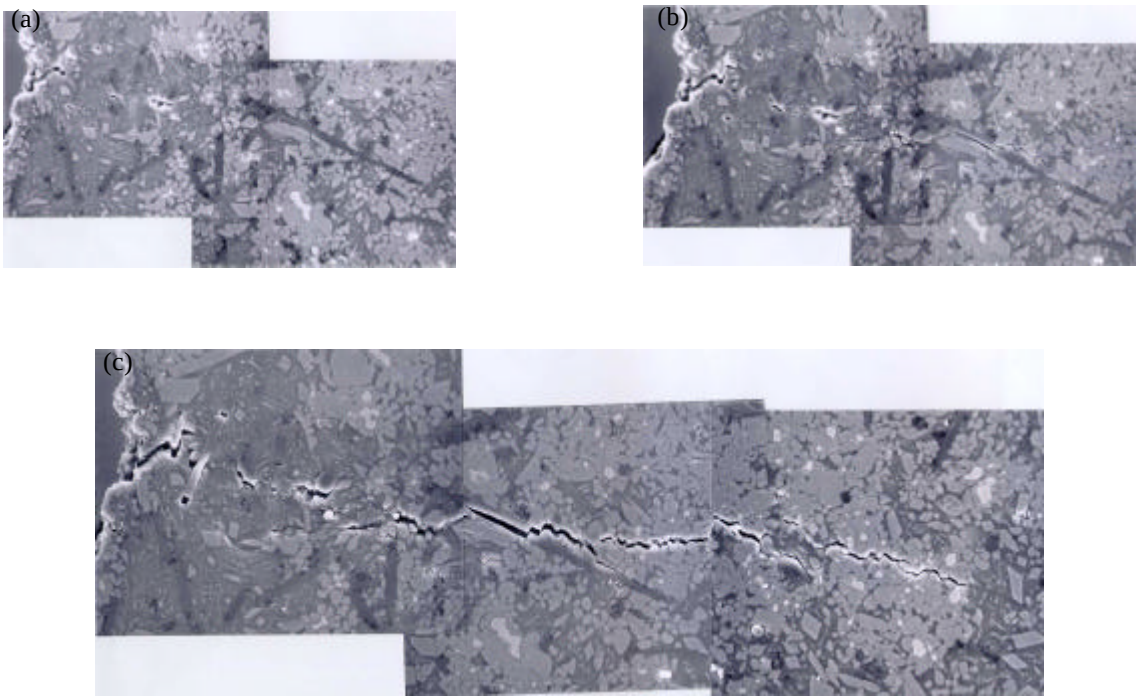

Fig. 8: A series of SEM micrographs near a notch tip of (10%Al_2O_3·SiO_2 + 5%Ni) / Al hybrid composite, showing : (a) microcrack formation by the separation of short fiber / matrix interface (K_Q=10.76 MPa$\sqrt{m}$), (b) (K_Q=11.16 MPa$\sqrt{m}$) and (c) crack propagation mainly along the intermetallic compound clusters

CONCLUSIONS

1. (10%Al_2O_3• SiO_2+5%Ni)/Al and (10%Al_2O_3• SiO_2+5%TiO_2)/Al hybrid composites were fabricated successfully by the reaction squeeze casting.
2. Al_3Ni intermetallic compounds and Al_3Ti intermetallic compounds were formed by the reaction of molten aluminum with Ni powder and TiO_2 powder.
3. Mechanical properties such as microhardness and flexural strength of hybrid composites were superior to those of (15%Al_2O_3• SiO_2)/Al composite. The enhancement of these mechanical properties is likely to be due to the hard intermetallic compound particles.
4. Tensile properties of (10%Al_2O_3• SiO_2+5%Ni)/Al hybrid composite were superior to that of (10%Al_2O_3• SiO_2+5%TiO_2)/Al hybrid composite at room temperature and 300 ^oC. The difference of mechanical properties was due to the amount of reaction product. Microstructural investigation showed that (10%Al_2O_3• SiO_2+5%Ni)/Al hybrid composite had more intermetallic compounds than (10%Al_2O_3• SiO_2+5%TiO_2)/Al hybrid composite.
5. It was identified from the in-situ fracture test of (15%Al_2O_3• SiO_2)/Al composite and (10%Al_2O_3• SiO_2+5%Ni)/Al hybrid composite that the microcrack initiation of both composite occurred at the short fiber/matrix interfaces. The microcrack of (15%Al_2O_3• SiO_2)/Al composite propagated mainly along the separated interfacial regions and shear bands were well developed in the matrix areas. The microcrack of (10%Al_2O_3• SiO_2+5%Ni)/Al hybrid composite propagated along the intermetallic compound clusters and fiber/matrix interfaces.

ACKNOWLEDGMENT

The authors would like to thank Prof. Sunghak Lee of Pohang University of Science and Technology for in-situ test and helpful discussions. This work was supported by RASOM(CNU).

REFERENCES

1. I. M. Park and B. S. Kim. 1996. *Bulletin of the Korean Inst. of Met. & Mat.*, 9(2): 112-125.
2. J. T. Blucher. 1992. *J. Mat. Pross. Tech.*, 30:381-390.
3. J. E. Allision and G. S. Cole. 1993. *J. of Metals*, :19.
4. M.G. Mckimpson and T. E. Scott. 1987. *Mat. Sci. and Eng.*,:93.
5. H. Fukunaga and G. K. Yeoh. 1992. *J. of Jpn. Soc. of Powd. and Powd. Met.*, 39(6):459-463.
6. I. Tsuchitori and H. Fukunaga. 1993. *Proc. ICCM-10*. :906-912.
7. S. S. Kim, S. M. Kang, S. J. Kim, I. K. Park and I. D. Choi. 1996. *Proc. ICCM-11*. :164-173.
8. H. Fukunaga. 1994. *J. of Soc. Mater. Sic.* Jpn., 43(4):373-381.
9. S. S. Kim, I. M. Park, S. J. Kim and I. D. Choi. 1997. *J. of the Korean Foundrymen's Society*, 17(4): 338-346.
10. E. K. Jeon, K.C. Kim, I. D. Choi and I. M. Park, 1996. *J. of the Korean Society for Composite Materials*, 9(2):12-22.
11. M. S. Kim, K. M. Cho, I. M. Park, 1994. *J. of the Korean Foundrymen's Society*, 14(3): 258-266.
12. S. H. Lee, K. S. Sohn, I. M. Park and K. M. Cho, 1995. *Metals and Materials*, 1(1):37-46.
13. C. G. Lee, S. H. Lee, D. I. Kwon and I. M. Park, 1993. *Scripta Metallurgica et Materialia*, 28:949-954.
14. K. S. Sohn, K. J. Euh, S. H. Lee and I. M. Park, 1998. *Metallurgical and Materials Transctions A*, 29A:2543-2554.
15. K. C. Kim, Y. S. Cho, S. H. Lee and I. M. Park, 1996. *J. of the Korean Foundrymen's Society*, 16(6): 537-549.
16. T. B. Massalski, 1958. *Binary Phase Diagram*, ASM, Metal Park, Ohio :142.
17. T. B. Massalski, 1958. *Binary Phase Diagram*, ASM, Metal Park, Ohio :175